AIMS Mathematics, 11(1): 2406–2429.
DOI: 10.3934/math.2026098
Received: 09 November 2025
Revised: 12 January 2026
Accepted: 19 January 2026
Published: 26 January 2026

http://www.aimspress.com/journal/Math

Research article

Energy balancing integrals, orthogonal polynomial systems, and matrix Lyapunov equations

Netzer Moriya*

siOnet - Applied Modeling Research, Edison, NJ, USA

* **Correspondence:** Email: netzer@si-o-net.com.

Abstract: Starting from a steady-state energy–balance law for noisy, linearly damped fields, we derive an operator covariance equation in Lyapunov–Sylvester form. On the unit disk with self-adjoint boundary conditions, the corresponding generator is diagonalized by the Zernike polynomials, and finite-mode projection yields a matrix Lyapunov equation for modal covariances. We prove explicit a priori truncation-error bounds tailored to Zernike systems: in the diagonal (or diagonally dominant) case the operator-norm tail admits a closed-form expression and, for Kolmogorov-type spectra, decays at a rate $O(N^{-7/3})$; for general Hilbert–Schmidt noise covariances we obtain Hilbert–Schmidt tail bounds with explicit dependence on system parameters and dissipation rates. We further extend the formulation to exponentially correlated (Ornstein-Uhlenbeck) forcing via an augmented-state Lyapunov/Sylvester construction, yielding closed-form denominator shifts and a covariance-based inversion for the OU correlation time τ. Numerical examples validate the Lyapunov solves, the derived error bounds, and the τ recovery procedure.

Keywords: energy balance; Lyapunov equations; Zernike polynomials; orthogonal polynomials; covariance operators; stochastic PDEs; Ornstein-Uhlenbeck processes
Mathematics Subject Classification: 15A24, 35R60, 42C05, 60H15, 93E03

1. Introduction: Energy-balance framework for steady-state covariance

Addressing the dynamics of spatially extended dissipative systems, such as atmospheric optics or plasma physics, often requires navigating complex stochastic processes and high-dimensional parameter spaces. Connecting between a system's fundamental physical principles and its tractable mathematical representation is paramount for predictive modeling and control. Our work tackles this challenge by establishing a framework where fundamental physical principles naturally motivate the mathematical structures used for analysis.

The interplay between mathematical structures and physical phenomena frequently reveals

profound connections.

Classical orthogonal polynomial systems – such as Zernike polynomials in optics [1], Hermite polynomials in quantum mechanics, and spherical harmonics in electromagnetism – emerge as eigenfunctions of differential operators governing fundamental processes. Concurrently, matrix Lyapunov equations are central to characterizing covariance evolution in stochastic systems, underpinning modern control theory and statistical mechanics [2, 3].

Classical covariance closures for stochastic PDEs continue to evolve along two complementary tracks. On the modeling side, recent SPDE frameworks refine how covariance operators arise and are approximated in bounded domains and finite elements, including fractional and nonstationary structures that map cleanly to linear operator forms used in our pipeline [4–6]. On the optics side, Zernike-based representations remain the lingua franca for phase statistics: recent studies revisit Zernike orthogonality under propagation, and propose hybrid Fourier–Zernike phase screens (and data-driven variants) to better emulate Kolmogorov-type spectra–developments that justify our choice of a Zernike spectral basis and inform the structure of Q [7–10]. Finally, large-scale covariance solvers based on Lyapunov/Sylvester equations have seen steady algorithmic progress: integrated Krylov–ADI schemes, projection methods for Sylvester equations, and low-rank ADI/Smith variants now target parameterized and discrete-time settings, which directly support our finite-mode truncations and OU-augmented blocks [11–14]. These strands together motivate our approach: a new Lyapunov formulation with Zernike specialization and OU forcing, solved via modern low-rank linear-matrix-equation methods.

This work presents a disk-adapted synthesis of classical connections between linear dissipative dynamics, steady-state covariances, and Lyapunov/Sylvester equations. We organize the development as a pipeline (see Figure 1) balance $\rightarrow$ geometry $\rightarrow$ finite solve: the steady-state balance motivates the covariance equation, geometry suggests working in eigenbases adapted to the domain (Zernike on the unit disk), and finite-mode truncation leads to a computable matrix Lyapunov system. Our contributions are in (i) specializing this pipeline to the disk/Zernike setting, (ii) deriving rigorous a priori truncation error bounds (operator and Hilbert–Schmidt), and (iii) extending the steady-state covariance construction to OU-colored forcing via an augmented-state Lyapunov formulation, including a covariance-based identification map for the OU correlation time τ.

It is useful to contrast this approach with standard numerical workflows for linear PDE/SPDE covariance computation. On general domains, steady-state covariances are often obtained either by simulating sample paths and estimating covariances by Monte Carlo, or by discretizing the associated operator Lyapunov equation on a grid (e.g., finite-element Lyapunov formulations for parabolic SPDEs [15]). In such grid-based settings the resulting matrix equations can be very large and typically require large-scale low-rank Lyapunov solvers (ADI/Krylov and related methods; see, e.g., [11,13,14]). In contrast, on the unit disk the Zernike basis diagonalizes the generator, so the steady covariance admits the entrywise representation $P_{jk} = Q_{jk}/(R_j + R_k)$, and our main focus becomes (i) casting physically meaningful noise models into the same basis and (ii) providing a priori truncation guidance via explicit error bounds.

1.1. Contributions (classical ingredients vs. new contributions)

- *Classical ingredients used:* Lyapunov/Sylvester characterization of steady-state covariances for linear dissipative systems, and the augmented-state Lyapunov formulation for OU (exponentially

correlated) forcing.

- *New contributions of this work:* (i) Zernike/disk-specialized truncation error bounds in operator and Hilbert–Schmidt norms, (ii) explicit disk-scaling laws using Zernike eigenvalue growth and Kolmogorov-type modal spectra; and (iii) structured incorporation of Kolmogorov-type forcing in the Zernike basis, together with an explicit distinction between exact symmetry/selection rules and practical modeling approximations.

We now summarize and present several rigorously quantified results, including:

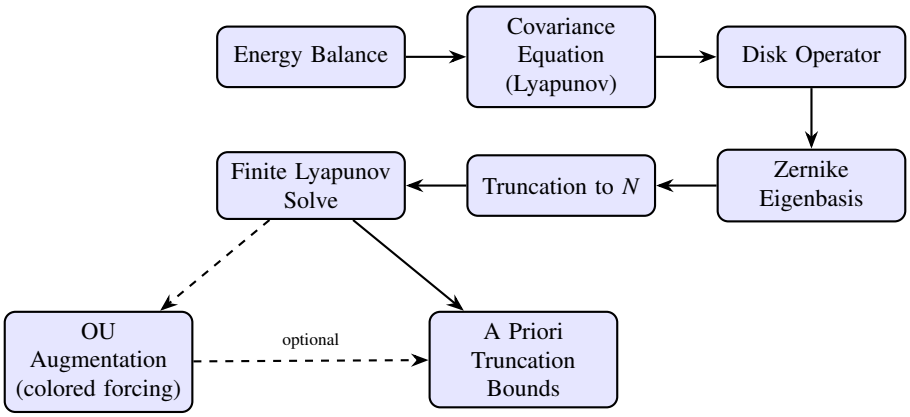

Figure 1. Schematic flow-chart of the analysis pipeline. The solid arrows give the core white-noise route; the dashed arrows show the optional OU-coloured-forcing branch that leads to the same a-priori bounds box but with modified denominators.

(1) We rigorously incorporate and leverage the known mode-coupling structure of realistic optical forcings, such as atmospheric turbulence (Kolmogorov model), by casting them as the noise operator Q directly in the Zernike basis. This concretely grounds the abstract operator in a physically observable phenomenon [16].

(2) We derive precise, disk-specific error bounds for finite-dimensional approximations of the steady-state covariance operator P. These bounds, explicitly tailored for Zernike systems, include the operator norm for diagonally dominant noise and the Hilbert-Schmidt norm for general noise. They detail their explicit dependence on system parameters (α, γ) and truncation order (N), and uniquely lead to explicit analytical rules for determining the required modal truncation order for a given accuracy.

Furthermore, we significantly extend this framework to handle both exponentially correlated (Ornstein-Uhlenbeck) forcing and generalized rational-transfer-function colored noise. This is achieved via an augmented-state Sylvester formulation, revealing a simple uniform denominator shift (or product of shifts for general rational noise) in modal covariance that preserves the pipeline structure. We also establish a new identifiability condition for noise correlation parameters directly from modal covariances.

2. The master energy dissipation framework

Consider a general stochastic dynamical system evolving on a separable Hilbert space $\mathcal{H}$ with inner product $\langle\cdot,\cdot\rangle$ and induced norm $\|\cdot\|$. The system is governed by the stochastic evolution equation:

$$\frac{\mathrm{d}u}{\mathrm{d}t} = \mathcal{L}u + \xi(t), \tag{2.1}$$

where $u(t) \in \mathcal{H}$.

Assumption 2.1 (Self-adjoint dissipative structure)**.** *The operator $\mathcal{L} : \mathcal{D}(\mathcal{L}) \subset \mathcal{H} \to \mathcal{H}$ is self-adjoint, densely defined, and strictly dissipative. Specifically, there exists $\gamma_0 > 0$ such that $\langle\phi, \mathcal{L}\phi\rangle \le -\gamma_0\|\phi\|^2$ for all $\phi \in \mathcal{D}(\mathcal{L})$. $\mathcal{L}$ possesses a complete orthonormal system of eigenfunctions $\{\phi_k\}_{k=1}^{\infty}$ with real eigenvalues $\{\lambda_k\}_{k=1}^{\infty}$ satisfying $\lambda_k \le -\gamma_0 < 0$.*

Assumption 2.2 (White-in-time stochastic forcing)**.** *The noise $\xi(t)$ is a white-in-time process characterized by its covariance structure via a positive, self-adjoint trace-class operator $Q : \mathcal{H} \to \mathcal{H}$: $\langle\langle\phi, \xi(t)\rangle\langle\psi, \xi(s)\rangle\rangle = \langle\phi, Q\psi\rangle\delta(t-s)$. Q represents the spatial (and instantaneous temporal) structure of energy injection.*

Proposition 2.1 (Steady-state energy covariance law)**.** *Under Assumptions 2.1 and 2.2, the unique, positive, self-adjoint steady-state energy covariance operator $P : \mathcal{H} \to \mathcal{H}$ solves the infinite-dimensional Lyapunov equation:*

$$\mathcal{L}P + P\mathcal{L} = -Q. \tag{2.2}$$

In the eigenbasis $\{\phi_k\}$ of $\mathcal{L}$, the matrix elements of P are:

$$(P)_{jk} = \langle\phi_j, P\phi_k\rangle = \frac{\langle\phi_j, Q\phi_k\rangle}{-(\lambda_j + \lambda_k)}. \tag{2.3}$$

For clarity, let $\delta_j := -\lambda_j > 0$ be the modal dissipation rates, and then $(P)_{jk} = (Q)_{jk}/(\delta_j + \delta_k)$.

Proof. The proof relies on standard results from infinite-dimensional stochastic systems theory, including the absolute convergence of the energy dissipation integral and properties of self-adjoint dissipative operators. Details are provided in Appendix A. □

3. Spectral reduction and finite-dimensional projections

Proposition 3.1 (Matrix Lyapunov system)**.** *Let Π_N be the orthogonal projection onto span$\{\phi_1, \ldots, \phi_N\}$. The finite-dimensional energy covariance $P_N = \Pi_N P \Pi_N$ is an $N \times N$ matrix with entries $(P_N)_{jk} = \langle\phi_j, P\phi_k\rangle$ for $j, k \in \{1, \ldots, N\}$. This matrix satisfies the finite-dimensional Lyapunov equation:*

$$\Lambda_N P_N + P_N \Lambda_N = -Q_N, \tag{3.1}$$

where $\Lambda_N = diag(\lambda_1, \ldots, \lambda_N)$ and $(Q_N)_{jk} = \langle\phi_j, Q\phi_k\rangle$ for $j, k \in \{1, \ldots, N\}$. The solution is explicitly given by $(P_N)_{jk} = \frac{(Q_N)_{jk}}{-(\lambda_j+\lambda_k)}$.

Remark 3.1. *The restriction to self-adjoint operators (Assumption 2.1) ensures real eigenvalues (physical decay rates) and a positive definite covariance matrix, which is fundamental for physical consistency.*

4. Geometric realization: Zernike polynomials on the unit disk

The unit disk is not merely a convenient example: it is a central application geometry in optics and wave-based systems. Circular apertures arise in telescope and microscope pupils (including adaptive optics), laser beams and resonators, and other disk-shaped sensing/actuation configurations. In these settings, Zernike modes provide a standard, geometry-adapted basis for representing spatial fields and their statistics, which motivates specializing the abstract Hilbert-space covariance framework to the disk.

In this work the Zernike basis arises because we model disk dynamics using a self-adjoint dissipative operator whose eigenfunctions are the Zernike modes; this is a modeling choice for tractability and disk geometry, not a logical necessity implied by energy balance alone.

We apply the framework to a field on the unit disk $D = \{(x, y) \in \mathbb{R}^2 : x^2 + y^2 \leq 1\}$, which is crucial for optical systems. The Hilbert space is $L^2(D, \mathrm{d}\mu)$ with the normalized area measure $\mathrm{d}\mu = \frac{1}{\pi}\, r\, \mathrm{d}r\, \mathrm{d}\theta$, making Zernike polynomials orthonormal.

From a modeling standpoint, we adopt a minimal dissipative operator that captures two generic physical effects for disk-defined fields: (i) linear relaxation/smoothing through a self-adjoint elliptic term (here realized by the Zernike operator $\mathcal{L}_Z$, which plays a Laplacian-like role on the disk), and (ii) uniform damping through the term $-\gamma u$. The parameter $\alpha > 0$ controls the strength of spatial smoothing (spectral roll-off), while $\gamma > 0$ sets a baseline decay rate. This choice is made for physical plausibility and computational tractability: it preserves self-adjoint dissipation and admits a disk-adapted eigenbasis (Zernike), enabling closed-form modal covariance structure and rigorous a priori truncation control. We emphasize that this is a modeling choice, not a uniquely derived law from first principles.

The system's dissipative dynamics, specifically, defines the operator $\mathcal{L}$ from Eq (2.1) in the form:

$$\mathcal{L}u = -\alpha^2 \mathcal{L}_Z u - \gamma u, \quad \text{so that} \quad \frac{\partial u}{\partial t} = -\alpha^2 \mathcal{L}_Z u - \gamma u + \xi(x, y, t), \tag{4.1}$$

where $\alpha > 0$ scales the spectral response, $\gamma > 0$ provides uniform dissipation, and $\xi(x, y, t)$ is white-in-time noise.

Theorem 4.1 (Zernike operator and eigenvalues)**.** *The (real) Zernike circle polynomials $Z_{nm}(x, y)$ (with radial degree n and azimuthal frequency m) are eigenfunctions of the differential operator $\mathcal{L}_Z f = -\frac{1}{r}\,\partial_l\Big(r(1 - r^2)\,\partial_r f\Big) - \frac{1}{r^2}\,\partial_{\theta\theta} f$, with natural boundary conditions. Their eigenvalues are [17]:*

$$\mathcal{L}_Z Z_{nm} = \mu_{nm} Z_{nm}, \quad \textit{where} \quad \mu_{nm} = n(n + 2) - m^2. \tag{4.2}$$

For valid Zernike indices ($n \geq |m|$, $n - |m|$ even), these eigenvalues are non-negative. The full dissipative operator $\mathcal{L} = -\alpha^2 \mathcal{L}_Z - \gamma I$ (from Eq (4.1)*) thus has eigenvalues:*

$$\lambda_{nm} = -\alpha^2 \mu_{nm} - \gamma. \tag{4.3}$$

As $\mu_{nm} \geq 0$, $\alpha^2 > 0$, and $\gamma > 0$, it follows that $\lambda_{nm} \leq -\gamma < 0$, satisfying Assumption 2.1. The least negative eigenvalue is $\lambda_{00} = -\gamma$ (piston mode, $\mu_{00} = 0$).

This theorem establishes that the Zernike polynomials form a physically natural eigenbasis for analyzing dissipative processes on a disk, a fundamental geometric step in our proposed pipeline.

Proof. See Appendix B for the derivation using polar coordinates and properties of Zernike radial polynomials. □

4.1. Energy covariance in the Zernike basis: Quantification of optical forcing

The general energy framework, when applied to the Zernike system, yields energy covariance matrix elements $(P)_{nm,n'm'} = (Q)_{nm,n'm'}/(\alpha^2(\mu_{nm} + \mu_{n'm'}) + 2\gamma)$. The structure of P (diagonal, block-diagonal, or full) is dictated by the spatial correlations of the noise operator Q. For optical systems, Q typically represents stochastic phase distortions from atmospheric turbulence.

Theorem 4.2 (Kolmogorov noise operator in the Zernike basis)**.** *For a phase perturbation $\xi(\mathbf{x}, t)$ following the Kolmogorov turbulence model on a circular aperture, Noll's seminal work [16] rigorously derived the mode-coupling structure of the noise operator Q in the Zernike basis $Z_j(\mathbf{x})$. Its matrix elements $(Q)_{jk} = \langle Z_j, QZ_k\rangle_\mu$ are proportional to $r_0^{-5/3}$ (Fried parameter) and exhibit a structured sparse form for statistically isotropic Kolmogorov turbulence:*

- $(Q)_{jk} = 0$ *if* $m_j \neq m_k$.
- $(Q)_{jk} = 0$ *if* $m_j = m_k$ *and* n_j *and* n_k *have different parity* ($n_j - n_k$ *is odd).*

This results in a block-diagonal structure for Q in the Zernike basis, reflecting inherent symmetries in the turbulence model. This rigorous quantification illustrates how Q is explicitly structured by physical parameters, with coupling primarily for lower modes, leading to efficient truncation.

Remark 4.1 (Exact versus modeling structure)**.** *The selection rules stated above (block structure in azimuthal frequency and parity constraints) are exact consequences of statistical isotropy on an ideal circular aperture for Kolmogorov turbulence. Additional simplifications often used in practice—such as near-diagonality, power-law proxies for modal variances, or empirically calibrated decay of off-diagonal couplings—are modeling approximations introduced for validation and tractable computation. In measured turbulence phase screens, finite-aperture and experimental effects can deviate from idealized symmetries (e.g., aperture obscurations, nonstationarity, finite outer scale, and measurement artifacts); therefore, the structured noise models used in this work should be understood as physically motivated approximations used to test the theory and demonstrate computational tractability.*

Proof. A detailed proof building on angular and radial symmetries of the Kolmogorov kernel is given in Appendix B. □

5. Exponentially correlated forcing via the augmented-state Sylvester law

Building on the white-in-time noise framework, we now significantly extend it to include temporally correlated forcing, specifically covering Ornstein-Uhlenbeck (OU) processes and generalized rational colored noise. This provides a more realistic representation for many physical systems where noise has a finite correlation time. Let $x(t) \in \mathcal{H}$ solve $\dot{x} = \mathcal{L}x + \eta$, where $\mathcal{L}$ is defined as in Section 4, and $\eta(t)$ is an OU process in $\mathcal{H}$ solving:

$$\mathrm{d}\eta = -\tau^{-1}\eta \, \mathrm{d}t + \sqrt{2\tau^{-1}}\, Q^{1/2} \, \mathrm{d}W_t. \tag{5.1}$$

Here, $\tau > 0$ is the correlation time, and Q is the stationary spatial covariance operator of $\eta(t)$ (meaning $\langle \eta\eta^* \rangle = Q$). We augment the state to $z = (x, \eta)$.

Theorem 5.1 (OU forcing preserves pipeline: Covariance shift)**.** *Assume $\mathcal{L}$ is self-adjoint and dissipative with eigenvalues $\{\lambda_j\}$ and $\tau > 0$. The steady covariance $\mathbb{P}$ of the augmented state $z = (x, \eta)$ solves $\mathbb{A}\mathbb{P} + \mathbb{P}\mathbb{A}^* = -\mathbb{G}\mathbb{G}^*$. For its P_{xx} block (the covariance of $x(t)$), the modal elements are given by:*

$$(P_{xx})_{jk} = \frac{(Q)_{jk}}{(-\lambda_j)(-\lambda_k)} \cdot \frac{(-\lambda_j - \lambda_k + 2\tau^{-1})}{((-\lambda_j + \tau^{-1})(-\lambda_k + \tau^{-1}))}. \tag{5.2}$$

If Q is diagonal in the eigenbasis of $\mathcal{L}$, meaning $(Q)_{jk} = q_j \delta_{jk}$, then $(P_{xx})_{jj}$ simplifies to:

$$(P_{xx})_{jj} = \frac{q_j}{(-\lambda_j)(-\lambda_j + \tau^{-1})}. \tag{5.3}$$

Proof. The proof involves setting up an augmented-state Lyapunov system and solving the resulting block equations. Details are given in Appendix C. □

Corollary 5.1 (Zernike specialization with OU forcing)**.** *With $\lambda_{nm} = -(\alpha^2 \mu_{nm} + \gamma)$, the diagonal modal covariance for Zernike systems under diagonal Q is:*

$$(P_{xx})_{nm,nm} = \frac{(Q)_{nm,nm}}{(\alpha^2 \mu_{nm} + \gamma)(\alpha^2 \mu_{nm} + \gamma + \tau^{-1})}. \tag{5.4}$$

Thus, exponentially correlated forcing introduces an additional uniform damping factor *of $(\cdot + \tau^{-1})$ in the covariance denominators. This effectively reflects how finite-bandwidth noise suppresses long-time power contributions to each mode, preserving the Zernike block structure (in azimuthal index m) inherited from the input Q.*

5.1. Identifiability and estimation of the correlation time τ

A crucial aspect of applying the OU-forced model is the ability to determine its correlation time τ from observational data. Here, we present a direct approach to identify and estimate τ from the steady-state modal variances, assuming modal noise strengths $q_j = (Q)_{jj}$ and system dissipation rates $R_j = -\lambda_j$ are known.

Estimating parameters of OU processes is classical when time series are available, including likelihood- and moment-based estimators under discrete or low-frequency sampling [18]. In high dimensions, a substantial literature focuses on estimating the drift (and related parameters) under structural assumptions such as sparsity [19, 20]. The viewpoint adopted here is complementary: we exploit the modal steady-state covariance formula to obtain a closed-form inversion for τ from stationary modal variances, which is useful when covariance information is available (or estimated) but long, finely sampled trajectories are not.

From Eq (5.3), for diagonal Q, the steady-state variance of mode j is given by:

$$(P_{xx})_{jj} = \frac{q_j}{R_j(R_j + \tau^{-1})}. \tag{5.5}$$

This equation can be rearranged to directly solve for τ^{-1}:

$$\tau^{-1} = \frac{q_j}{R_j(P_{xx})_{jj}} - R_j. \tag{5.6}$$

This formula demonstrates that the inverse correlation time τ^{-1} is point-identifiable from a single mode j (provided $q_j > 0$, $(P_{xx})_{jj} > 0$, and $R_j > 0$). It leverages steady-state variances directly, rather than relying on full time-lagged autocovariance functions, which are generally more complex for output processes driven by OU noise. A more robust estimator for τ can be obtained by aggregating across a set $\mathcal{J}$ of sufficiently excited modes, for example, by computing a weighted average:

$$\widehat{\tau^{-1}} \;=\; \frac{\sum_{j\in\mathcal{J}} w_j \left(\frac{q_j}{R_j (P_{xx})_{jj}} - R_j\right)}{\sum_{j\in\mathcal{J}} w_j}, \tag{5.7}$$

with appropriate weights w_j (e.g., inversely proportional to the variance of the estimate for each mode, or signal-to-noise ratio-based choices). This provides a simple, closed-form identification procedure for τ within the established modal OU theory. A practical choice of weights can be justified by uncertainty propagation. If the modal variances $(P_{xx})_{jj}$ are estimated with approximately mode-independent relative error, then the induced uncertainty in the per-mode inversion $\hat{\tau}_j^{-1} = \frac{q_j}{R_j (P_{xx})_{jj}} - R_j$ scales like $(P_{xx})_{jj}^{-1}$, and inverse-variance weighting suggests $w_j \propto (P_{xx})_{jj}^2$. More generally, any monotone signal-to-noise proxy (e.g., $w_j \propto (P_{xx})_{jj}$) emphasizes well-excited modes; the trimming step is included only to remove nonphysical inversions that may arise from noisy covariance estimates.

Numerical robustness. While the inversion map $\tau^{-1} = \frac{q_j}{R_j (P_{xx})_{jj}} - R_j$ is exact under the model assumptions, it can be numerically ill-conditioned for modes with small $(P_{xx})_{jj}$ or when $(P_{xx})_{jj}$ is estimated with substantial noise. Uncertainty in q_j (forcing calibration) and in R_j (dissipation rates) propagates directly into $\hat{\tau}$ through the same formula. For practical estimation we therefore recommend: (i) using multiple well-excited modes (thresholding or excluding very small variances), (ii) robust aggregation across modes (trimmed mean/median-type estimators and discarding nonphysical inversions with $\hat{\tau}_j^{-1} \le 0$), and (iii) signal- or inverse-variance-type weights (as motivated above by uncertainty propagation). The sensitivity experiment in Section 7 (Figure 3(b)) provides an empirical illustration of how $\hat{\tau}$ degrades as multiplicative noise increases.

5.2. General rational colored forcing via companion augmentation

We extend the OU case to a general temporally colored forcing whose scalar transfer function is a stable rational

$$H(s) \;=\; \sum_{i=1}^{p} \frac{\beta_i}{s + a_i}, \qquad a_i > 0,\ \beta_i \in \mathbb{R}, \tag{5.8}$$

so that the forcing takes the form $\eta(t) = \sum_{i=1}^{p} \eta_i(t)$ with

$$\dot{\eta}_i(t) = -a_i\, \eta_i(t) + \sqrt{2a_i}\, Q^{1/2} \dot{W}_i(t), \qquad i = 1, \dots, p, \tag{5.9}$$

and mutually independent Wiener processes W_i. Define the augmented state $z = [\, x, \eta_1, \dots, \eta_p \,]^\top$ and operators

$$\mathbb{A} \;=\; \begin{bmatrix} \mathcal{L} & I & I & \cdots & I \\ 0 & -a_1 I & 0 & \cdots & 0 \\ 0 & 0 & -a_2 I & \cdots & 0 \\ \vdots & \vdots & \vdots & \ddots & \vdots \\ 0 & 0 & 0 & \cdots & -a_p I \end{bmatrix}, \qquad \mathbb{G} \;=\; \begin{bmatrix} 0 \\ \sqrt{2a_1}\, Q^{1/2} \\ \sqrt{2a_2}\, Q^{1/2} \\ \vdots \\ \sqrt{2a_p}\, Q^{1/2} \end{bmatrix}. \tag{5.10}$$

Let $\mathbb{P} = \mathbb{E}[zz^*]$ with blocks $P_{x\eta_i}$ and $P_{\eta_i\eta_j}$. The augmented Lyapunov equation $\mathbb{A}\mathbb{P} + \mathbb{P}\mathbb{A}^* + \mathbb{G}\mathbb{G}^* = 0$ yields:

$$(-a_iI)P_{\eta_i\eta_i} + P_{\eta_i\eta_i}(-a_iI) + 2a_iQ = 0 \;\Rightarrow\; P_{\eta_i\eta_i} = Q, \tag{5.11}$$

$$\mathcal{L}P_{x\eta_i} + P_{x\eta_i}(-a_iI) + P_{\eta_i\eta_i} = 0 \;\Rightarrow\; P_{x\eta_i} = -(\mathcal{L} - a_iI)^{-1}Q, \tag{5.12}$$

$$\mathcal{L}P_{xx} + P_{xx}\mathcal{L}^* + \sum_{i=1}^{p}\left(P_{x\eta_i} + P_{\eta_i x}\right) = 0. \tag{5.13}$$

Hence, the covariance P_{xx} solves the Lyapunov equation with a modified forcing:

$$\mathcal{L}P_{xx} + P_{xx}\mathcal{L}^* + \widetilde{Q}_{\{a_i\}} = 0, \quad \widetilde{Q}_{\{a_i\}} := \sum_{i=1}^{p}\Big[(\mathcal{L} - a_iI)^{-1}Q + Q(\mathcal{L}^* - a_iI)^{-1}\Big]. \tag{5.14}$$

In the Zernike basis, writing $\mathcal{L}Z_j = \lambda_j Z_j$, we obtain the modal formula:

$$(P_{xx})_{jk} \;=\; \frac{\displaystyle\sum_{i=1}^{p}\Big(\frac{Q_{jk}}{\lambda_j - a_i} + \frac{Q_{jk}}{\overline{\lambda_k} - a_i}\Big)}{-(\lambda_j + \overline{\lambda_k})}. \tag{5.15}$$

In particular, if Q is diagonal and $\lambda_j \in \mathbb{R}$,

$$P_{jj} \;=\; \frac{q_j}{-\lambda_j}\sum_{i=1}^{p}\frac{1}{-\lambda_j + a_i}, \tag{5.16}$$

which exhibits a sum of generalized denominator shifts a_i. The simple product generalization of the OU shift would hold if the rational noise was modeled differently (e.g., as a cascaded filter of white noise), but for the adopted model of summed independent OU processes, it is a sum.

6. Mathematical structure and rigorous error bounds

Related numerical literature. Large-scale algebraic Lyapunov and Sylvester equations are the subject of extensive numerical literature, including low-rank ADI and projection/Krylov-type methods and their variants [11, 13, 14]. In addition, recent work has considered differential Lyapunov equations and fractional differential Sylvester/Lyapunov equations with dedicated time-stepping and Krylov-based approaches [21–23]. Our contribution is complementary to these general-purpose solvers: we leverage the disk-adapted Zernike eigenbasis to expose closed-form covariance structure and to derive explicit a priori truncation bounds tailored to disk geometry.

Notation. We use cumulative indexing $j \leftrightarrow (n_j, m_j)$ for Zernike modes, and write μ_j for the corresponding eigenvalues of the disk operator (Section 4). The modal decay rates are $R_j := \alpha^2\mu_j + \gamma$. In the Zernike basis, $Q_{jk} := \langle Z_j, QZ_k\rangle_\mu$ denotes noise-covariance entries, and in the diagonal case $q_j := Q_{jj} = \langle Z_j, QZ_j\rangle_\mu$. For truncation level N, Π_N denotes projection onto the first N modes and $P_N := \Pi_N P \Pi_N$. We also use the complement index set $\Omega_N := \{(j,k) \in \mathbb{N}^2 : \max(j,k) > N\}$ to describe residual tails.

We establish rigorous error bounds for finite-dimensional Zernike approximations. These bounds explicitly characterize the approximation quality for various noise structures and are crucial for the practical implementation of modal control systems. The formulation extends verbatim to the OU-forced setting by replacing $-(\lambda_j + \lambda_k)$ with the more complex denominator structure of Eq (5.2) and appropriately interpreting Q.

Remark 6.1 (Zernike mode indexing and eigenvalue growth)**.** *On the unit disk, Zernike modes Z_{nm} satisfy the eigenvalue relation $\mathcal{L}_Z Z_{nm} = \mu_{nm} Z_{nm}$ with $\mu_{nm} = n(n+2) - m^2$ (see Eq* (4.2)*). Under cumulative indexing $j \leftrightarrow (n_j, m_j)$ (e.g., Noll-like [16]), the number of modes up to radial degree n scales as $\sim (n+1)(n+2)/2$, so $n_j \simeq c\sqrt{j}$. For admissible indices ($n \geq |m|$ and $n - |m|$ even), $\mu_{nm} \geq n(n+2) - n^2 = 2n$, hence the minimal eigenvalue at radial degree n is $\mu_n^{\min} = 2n$ and therefore*

$$\mu_j^{\min} := \min_{m:\,(n_j,m)\ admissible} \mu_{n_j m} \simeq C_\mu \sqrt{j}. \tag{6.1}$$

Consequently, $\alpha^2 \mu_{N+1}^{\min} + \gamma = O(\alpha^2 \sqrt{N} + \gamma)$, and similarly $\delta_N := \min_{(j,k)\in\Omega_N} (\alpha^2(\mu_j + \mu_k) + 2\gamma) = O(\alpha^2 \sqrt{N} + \gamma)$.

Remark 6.2 (Scope of disk-scaling rates)**.** *Any explicit rate statements obtained by combining tail assumptions on Q (or on the diagonal spectrum q_j) with eigenvalue growth rely on the Zernike eigenvalue formula and the chosen cumulative indexing on the disk. The same derivation does not transfer verbatim to arbitrary orthogonal systems on other domains without re-checking the spectral growth and the indexing geometry.*

Theorem 6.1 (Zernike operator-norm truncation error)**.** *Let P be the (infinite-dimensional) steady-state covariance and $P_N = \Pi_N P \Pi_N$, its N-mode projection. Write $R_j := \alpha^2 \mu_j + \gamma$ and define $\mu_{N+1}^{\min} := \min_{j>N} \mu_j$.*

(1) ***Exact diagonal-Q case (equality).*** *If Q is diagonal in the Zernike basis, i.e., $Q_{jk} = q_j \delta_{jk}$, with $q_j = \langle Z_j, QZ_j \rangle_\mu \geq 0$, then*

$$\|P - P_N\|_{op} = \sup_{j>N} \langle Z_j, PZ_j \rangle_\mu = \sup_{j>N} \frac{q_j}{2R_j} = \sup_{j>N} \frac{q_j}{2(\alpha^2 \mu_j + \gamma)}. \tag{6.2}$$

(2) ***Controlled off-diagonal case (explicit assumption).*** *Decompose $Q = Q_{\text{diag}} + Q_{\text{off}}$, where Q_{diag} is diagonal in the Zernike basis, and let $Q_{\text{off,rest}} := (Q_{\text{off}})|_{\Omega_N}$ denote the off-diagonal residual restricted to $\Omega_N = \{(j,k) : \max(j,k) > N\}$. If there exists $\varepsilon_N \geq 0$ such that*

$$\|Q_{\text{off,rest}}\|_{op} \leq \varepsilon_N \sup_{j>N} q_j, \tag{6.3}$$

then the truncation tail satisfies the explicit bound

$$\|P - P_N\|_{op} \leq \frac{\sup_{j>N} q_j + \|Q_{\text{off,rest}}\|_{op}}{2(\alpha^2 \mu_{N+1}^{\min} + \gamma)} \leq \frac{(1+\varepsilon_N) \sup_{j>N} q_j}{2(\alpha^2 \mu_{N+1}^{\min} + \gamma)}. \tag{6.4}$$

In particular, when Q is diagonal-dominant in the sense of Eq (6.3) *with small ε_N, the operator-norm tail is controlled by the diagonal spectrum.*

(3) ***Rate statements under additional assumptions.*** *If* $\mu_{N+1}^{\min} \sim C_\mu \sqrt{N}$ *(Remark 6.1) and* $\sup_{j>N} q_j = O(N^{-p})$*, then*

$$\|P - P_N\|_{op} = O(N^{-(p+1/2)}). \tag{6.5}$$

For Kolmogorov-type modal spectra in cumulative indexing, $\sup_{j>N} q_j = O(N^{-11/6})$*, hence* $\|P - P_N\|_{op} = O(N^{-(11/6+1/2)}) = O(N^{-7/3})$.

Proof. The proof involves analysis of the spectral representation of P and careful partitioning of the operator into truncated and untruncated parts. Full details are provided in Appendix D. □

Theorem 6.2 (Zernike Hilbert–Schmidt truncation error)**.** *Assume* $Q \in HS(\mathcal{H})$ *(Hilbert–Schmidt). Then the Hilbert–Schmidt truncation tail admits the exact identity*

$$\|P - P_N\|_{HS}^2 = \sum_{(j,k)\in\Omega_N} \frac{|Q_{jk}|^2}{\left(\alpha^2(\mu_j + \mu_k) + 2\gamma\right)^2}, \qquad \Omega_N = \{(j,k) \in \mathbb{N}^2 : \max(j,k) > N\}. \tag{6.6}$$

Consequently, defining

$$Q_{\text{rest}} := Q|_{\Omega_N}, \qquad \delta_N := \min_{(j,k)\in\Omega_N} (\alpha^2(\mu_j + \mu_k) + 2\gamma), \tag{6.7}$$

we obtain the practical bound

$$\|P - P_N\|_{HS} \le \frac{\|Q_{\text{rest}}\|_{HS}}{\delta_N}. \tag{6.8}$$

Any simplified rate statement (e.g., $\|Q_{\text{rest}}\|_{HS} = O(N^{-\beta})$*) is an* assumption *about the forcing tail motivated by a specific noise model; combined with* $\delta_N = O(\alpha^2\sqrt{N}+\gamma)$ *(Remark 6.1), such assumptions yield corresponding algebraic convergence rates for* $\|P - P_N\|_{HS}$.

Proof. The Hilbert-Schmidt norm directly sums squared entries of the operator. The proof details the decomposition of $P - P_N$ and utilizes the spectral representation. Full details are provided in Appendix D. □

Remark 6.3 (Physical interpretation of convergence)**.** *The derived bounds explicitly show dependence on key system parameters: large* γ *(uniform dissipation) and large* α^2 *(geometric scaling of spatial dissipation) both enhance convergence by increasing modal dissipation. Critically, convergence rates depend on the decay of noise modal contributions (*q_j *or* $(Q)_{jk}$*), with structured noise (Theorem 4.2) enabling significantly higher rates. These results provide quantitative guidance for designing Zernike-based modal control systems by predicting the necessary truncation order for a given accuracy.*

6.1. A priori truncation index for a target tolerance

Assume Q is diagonal in the Zernike basis with $q_j \searrow 0$ and let μ_j denote the Zernike eigenvalues of $\mathcal{L}_Z$ ordered nondecreasingly. From $P_{jj} = q_j/(2(\alpha^2\mu_j + \gamma))$ (white-in-time case), the tail operator error equals $\|P - P_N\|_{\text{op}} = \sup_{j>N} P_{jj}$. Hence any N satisfying

$$\sup_{j>N} \frac{q_j}{2(\alpha^2\mu_j + \gamma)} \le \varepsilon \tag{6.9}$$

achieves $\|P-P_N\|_{\mathrm{op}} \le \varepsilon$. If $q_j \le C_q\, j^{-p}$ with $p > 0$ and $\mu_j \ge C_\mu \sqrt{j}$ (Zernike growth), then the monotone envelope yields

$$\|P - P_N\|_{\mathrm{op}} \;\le\; \frac{C_q}{2(\alpha^2 C_\mu \sqrt{N} + \gamma)}\, N^{-p} \;\le\; \varepsilon, \tag{6.10}$$

which implies the explicit design rule

$$N \;\ge\; \left(\frac{C_q}{2\varepsilon}\right)^{\frac{2}{2p+1}} \left(\frac{1}{\alpha^2 C_\mu}\right)^{\frac{2}{2p+1}} \quad \text{(dominant } \alpha^2 C_\mu \sqrt{N} \gg \gamma \text{ regime)}. \tag{6.11}$$

For OU forcing with correlation time τ, $P_{jj} = q_j/[(\alpha^2\mu_j + \gamma)(\alpha^2\mu_j + \gamma + \tau^{-1})]$ and the same argument gives

$$\|P - P_N\|_{\mathrm{op}} \;\le\; \sup_{j>N} \frac{q_j}{(\alpha^2\mu_j + \gamma)(\alpha^2\mu_j + \gamma + \tau^{-1})} \;\le\; \varepsilon, \tag{6.12}$$

leading to a more favorable $N(\varepsilon)$ due to the additional uniform shift τ^{-1} in the denominator.

7. Results and examples

7.1. Numerical protocol and reference configuration

To validate the theoretical results, we compute steady-state covariances in the Zernike eigenbasis under white and colored forcing and compare *empirical* truncation errors to the bounds derived in Theorems 6.1 and 6.2. Throughout, $R_j = \alpha^2\mu_j + \gamma$ denotes the (positive) decay rate associated with the jth Zernike mode, where μ_j is the corresponding eigenvalue of the Zernike operator on the disk.

For a truncation level N, we denote by Π_N the projection onto the first N Zernike modes (cumulative/Noll-like indexing) and define $P_N := \Pi_N P \Pi_N$. We also define the complement index set

$$\Omega_N := \{(j,k) \in \mathbb{N}^2 :\ \max(j,k) > N\}. \tag{7.1}$$

Since the infinite-dimensional P is not available in closed form for general non-diagonal forcing, we compute a high-resolution reference solution at size N_{ref} and measure truncation errors relative to this reference:

$$P_{\mathrm{ref}} := P_{N_{\mathrm{ref}}}, \quad E_{\mathrm{op}}(N) := \|P_{\mathrm{ref}} - P_N\|_{\mathrm{op}}, \quad E_{\mathrm{HS}}(N) := \|(P_{\mathrm{ref}} - P_N)|_{\Omega_N}\|_{\mathrm{HS}}. \tag{7.2}$$

(Here, $|_{\Omega_N}$ denotes a restriction to index pairs $(j,k) \in \Omega_N$.)

Unless otherwise stated, we use $N_{\mathrm{ref}} = 600$ and truncations $N \in \{50, 100, 150, 200, 300, 400, 500\}$, with parameters

$$\alpha = 1, \quad \gamma = 0.5, \quad \tau = 1.5, \tag{7.3}$$

and we exclude the piston mode ($j = 1$) from the forcing for clarity in the spectral tails.

7.2. White-noise case: Kolmogorov-type forcing and operator-norm equality

We first consider white-in-time forcing with a Kolmogorov-type spectrum in the Zernike basis. The Kolmogorov operator in Zernike coordinates is not perfectly diagonal; rather, it exhibits a structured mode-coupling pattern dictated by isotropy and Zernike symmetries (Theorem 4.2). To isolate and

visually validate the sharp operator-norm truncation statement of Theorem 6.1, we use a standard diagonal Kolmogorov-type proxy with modal variances

$$q_j \propto (n_j + 1)^{-11/3}, \tag{7.4}$$

where n_j is the radial degree of the jth Zernike mode. (The next subsection addresses genuinely non-diagonal Q consistent with Theorem 4.2).

Remark 7.1 (Proxy versus full Kolmogorov structure)**.** *In the diagonal experiment below we use a standard diagonal Kolmogorov-type proxy for q_j to isolate and visually validate the sharp operator-norm tail statement. This proxy should not be interpreted as asserting that the full Kolmogorov covariance is diagonal in Zernike coordinates; rather, the exact symmetry/selection rules are described in Theorem 4.2, and the subsequent non-diagonal experiments illustrate the truncation bounds in genuinely coupled power-spectral-density (PSD), Hilbert–Schmidt settings.*

For the diagonal generator $L = -\mathrm{diag}(R_1, \dots)$, the steady covariance P solves the Lyapunov equation

$$LP + PL = -Q, \tag{7.5}$$

and admits the closed-form entries

$$P_{jk} = \frac{Q_{jk}}{R_j + R_k}. \tag{7.6}$$

We compute P_N in two ways: (i) by solving the truncated Lyapunov equation (Eq (3.1)), truncated at N), and (ii) by evaluating Eq (7.6) on the truncated block. These agree to machine precision for each tested N.

Validation of Theorem 6.1 (operator norm, diagonal Q). In the diagonal case, Theorem 6.1 implies an equality for the operator-norm truncation tail:

$$\|P - P_N\|_{\mathrm{op}} = \sup_{j>N} \langle Z_j, PZ_j \rangle_\mu = \sup_{j>N} \frac{q_j}{2R_j}. \tag{7.7}$$

Figure 2(a) shows a log–log plot of the measured operator-norm tail $E_{\mathrm{op}}(N) = \|P_{\mathrm{ref}} - P_N\|_{\mathrm{op}}$ overlaid with the theoretical curve $B_{\mathrm{op}}(N) = \sup_{j>N} \frac{q_j}{2R_j}$. The two curves coincide across all tested truncations, confirming Eq (7.7). Table 1 reports representative values and the ratio $E_{\mathrm{op}}(N)/B_{\mathrm{op}}(N) \equiv 1$ (numerically exact in this experiment).

Table 1. Representative operator-norm truncation values in the diagonal Kolmogorov-type experiment. The ratio $E_{\mathrm{op}}(N)/B_{\mathrm{op}}(N) = 1$ for all tested N, validating the equality form of Theorem 6.1.

N	$E_{\mathrm{op}}(N)$	$B_{\mathrm{op}}(N)$	E/B
50	5.82×10^{-6}	5.82×10^{-6}	1.000
200	2.20×10^{-7}	2.20×10^{-7}	1.000
500	2.42×10^{-8}	2.42×10^{-8}	1.000

7.3. White-noise case: non-diagonal PSD forcing and Hilbert–Schmidt bounds

We next validate the general Hilbert–Schmidt truncation theory with non-diagonal PSD, HS noise covariances Q in the Zernike basis. Theorem 4.2 implies that physically realistic Kolmogorov forcing is structured (block-diagonal in azimuthal frequency and constrained by Zernike symmetries). Motivated by this, we test two distinct non-diagonal models:

(1) **Structured HS model (Kolmogorov symmetry proxy).** Off-diagonal couplings are permitted only between modes with the same azimuthal frequency and matching radial parity (consistent with the selection rules in Theorem 4.2), and decay with radial-degree separation. In the present configuration, the off-diagonal HS mass fraction is $\|Q - \mathrm{diag}(Q)\|_{\mathrm{HS}}/\|Q\|_{\mathrm{HS}} \approx 0.43\%$.

(2) **General HS model (broad but decaying couplings).** Off-diagonal couplings are broadly present and decay with index distance. Here, the off-diagonal HS mass fraction is $\|Q - \mathrm{diag}(Q)\|_{\mathrm{HS}}/\|Q\|_{\mathrm{HS}} \approx 2.95\%$.

Both models share the same diagonal spectrum (Kolmogorov-type q_j), but differ in their correlation structure; in particular, their relative HS difference satisfies $\|Q^{(\mathrm{gen})} - Q^{(\mathrm{str})}\|_{\mathrm{HS}}/\|Q^{(\mathrm{str})}\|_{\mathrm{HS}} \approx 2.94\%$.

In both cases, since the generator remains diagonal in the Zernike basis, we compute the steady covariance P by solving the truncated Lyapunov equation and (equivalently) by evaluating the closed form of Eq (7.6) at the chosen truncation.

Validation of Theorem 6.2 (Hilbert–Schmidt tail bound). Theorem 6.2 yields an HS truncation bound of the form

$$\|P - P_N\|_{\mathrm{HS}} \le \frac{\|Q_{\mathrm{rest}}\|_{\mathrm{HS}}}{\delta_N}, \qquad \delta_N := \min_{(j,k)\in\Omega_N} (\alpha^2(\mu_j + \mu_k) + 2\gamma), \tag{7.8}$$

where Q_{rest} denotes the restriction of Q to Ω_N. Figures 2(b) and 3(a) show the measured HS tail $E_{\mathrm{HS}}(N) = \|(P_{\mathrm{ref}} - P_N)|_{\Omega_N}\|_{\mathrm{HS}}$ overlaid with the theoretical bound $B_{\mathrm{HS}}(N) = \|Q_{\mathrm{rest}}\|_{\mathrm{HS}}/\delta_N$. In both noise models the bound holds across all tested truncations, with ratios $E_{\mathrm{HS}}(N)/B_{\mathrm{HS}}(N)$ in the range ≈ 0.14–0.27.

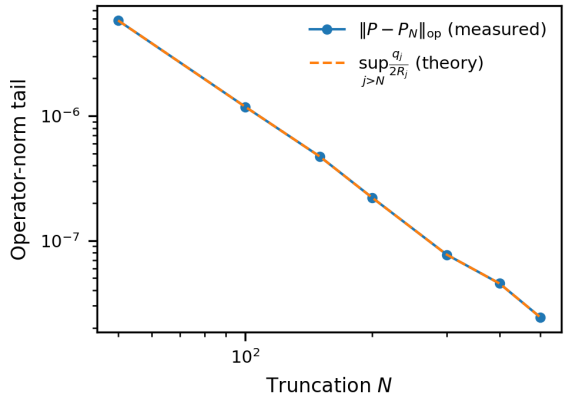

(a) Diagonal Kolmogorov-type proxy: $E_{op}(N)$ vs. $B_{op}(N)$ (Theorem 6.1 equality).

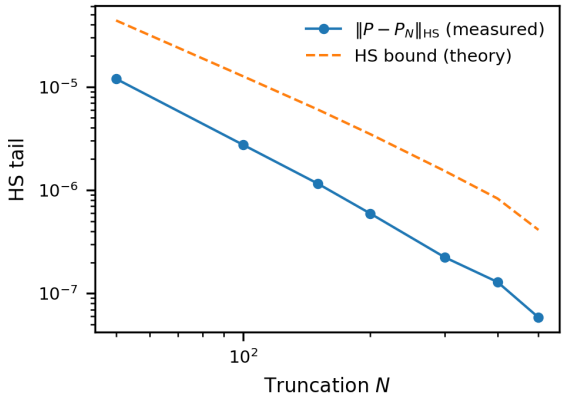

(b) Structured non-diagonal PSD, HS Q (Kolmogorov symmetry proxy): $E_{HS}(N)$ vs. $B_{HS}(N)$ (Theorem 6.2).

Figure 2. White-noise validation of truncation theory in the Zernike basis. (a) Diagonal Kolmogorov-type proxy: the measured operator-norm tail $E_{op}(N)$ coincides with the theoretical curve $B_{op}(N) = \sup_{j>N} \frac{q_j}{2R_j}$, confirming the equality case of Theorem 6.1. (b) Structured non-diagonal PSD, HS forcing consistent with the symmetry constraints of Theorem 4.2: the measured HS tail stays strictly below the theoretical bound $B_{HS}(N) = \|Q_{rest}\|_{HS}/\delta_N$ from Theorem 6.2.

7.4. OU colored-noise case: Augmented Lyapunov solution and τ identifiability

We finally consider colored forcing modeled by an OU process with correlation time τ. Following Section 5 of the paper, we form the augmented state and solve a finite-dimensional Lyapunov equation in the augmented space to obtain the stationary covariance block P_{xx}.

Validation of the augmented-state covariance formula. For diagonal $Q = \mathrm{diag}(q_j)$, the diagonal entries admit the closed-form expression (cf. Eq (5.3) and Corollary 5.1):

$$(P_{xx})_{jj} = \frac{q_j}{R_j\,(R_j + \tau^{-1})}. \tag{7.9}$$

Our augmented-state Lyapunov computation matches this closed form to machine precision in the tested configuration (relative error $\approx 10^{-16}$), confirming correctness of the OU formulation and its numerical implementation.

Validation of τ recovery. We validate the identifiability mapping in Section 5.1 via the per-mode inversion

$$\tau^{-1} = \frac{q_j}{R_j (P_{xx})_{jj}} - R_j, \tag{7.10}$$

and recover τ from synthetic $(P_{xx})_{jj}$ values. To mimic estimation uncertainty, we perturb $(P_{xx})_{jj}$ by multiplicative noise and aggregate the resulting $\hat{\tau}_j^{-1}$ robustly: we discard nonphysical values with $\hat{\tau}_j^{-1} \le 0$, apply a trimmed mean, and use signal weights proportional to $(P_{xx})_{jj}$. Figure 3(b) reports the recovered $\hat{\tau}$ versus the noise level. As expected, the mapping recovers τ accurately in the noise-free and small-noise regimes; at larger noise the estimate degrades, providing a quantitative sensitivity assessment of the procedure.

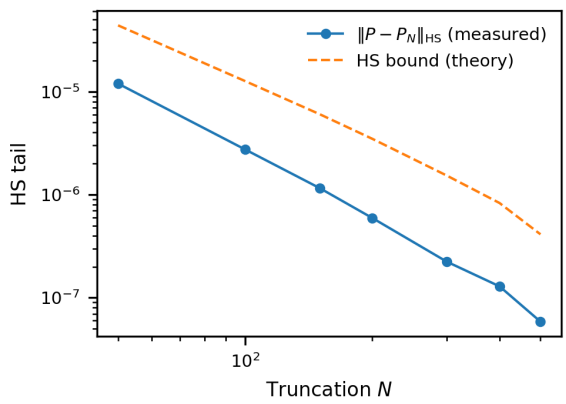

(a) General non-diagonal PSD, HS Q: $E_{\mathrm{HS}}(N)$ vs. $B_{\mathrm{HS}}(N)$ (Theorem 6.2).

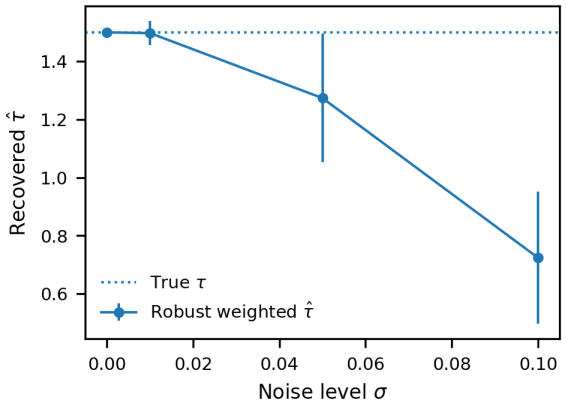

(b) OU forcing: recovered $\hat{\tau}$ vs. multiplicative noise level on synthetic $(P_{xx})_{jj}$.

Figure 3. Additional validations beyond the diagonal setting. (a) A broadly coupled (yet HS) non-diagonal PSD noise model also satisfies the HS truncation bound of Theorem 6.2 across all tested truncations. (b) OU colored-noise validation: the identifiability map from Section 5.1 recovers the true τ accurately in the noise-free and small-noise regimes; the plot quantifies degradation at higher noise levels.

8. Conclusions

This paper develops a disk-adapted synthesis of classical connections between linear dissipative dynamics, steady-state covariances, and Lyapunov/Sylvester equations, and provides rigorous quantification for Zernike systems on the unit disk.

Our main results include:

- *Zernike-specialized steady covariance construction:* For the unit disk, the Zernike eigenbasis yields a direct modal representation of steady covariances via finite-dimensional Lyapunov equations.

- *Quantified truncation control:* We prove explicit a priori truncation-error bounds for Zernike covariance truncations in both operator and Hilbert–Schmidt norms. In particular, for diagonal Kolmogorov-type spectra the operator-norm tail decays as $O(N^{-7/3})$, enabling principled selection of truncation order for a target accuracy.

- *OU-colored forcing and identifiability:* We extend the steady-state covariance formulation to exponentially correlated (OU) forcing via an augmented-state Lyapunov/Sylvester construction, yielding closed-form denominator shifts and a covariance-based inversion map for the OU correlation time τ.

Finally, the numerical examples in Section 7 validate the Lyapunov solves, confirm the sharp diagonal operator-norm tail formula, verify the Hilbert–Schmidt truncation bounds for non-diagonal PSD forcing models, and demonstrate τ recovery from synthetic modal covariance data.

Use of Generative-AI tools declaration

The author declares he has not used Artificial Intelligence (AI) tools in the creation of this article.

Conflict of interest

The author declares no conflict of interest.

References

1. M. Born, E. Wolf, *Principles of optics*, 7 Eds., Cambridge: Cambridge University Press, 1999.
2. G. Da Prato, J. Zabczyk, *Stochastic equations in infinite dimensions*, Cambridge: Cambridge University Press, 2010. https://doi.org/10.1017/CBO9780511666223
3. R. F. Curtain, H. Zwart, *An introduction to infinite-dimensional linear systems theory*, New York: Springer, 1995. https://doi.org/10.1007/978-1-4612-4224-6
4. L. Clarotto, D. Allard, T. Romary, N. Desassis, The SPDE approach for spatio-temporal datasets with advection and diffusion, *Spat. Stat.*, **62** (2024), 100847. https://doi.org/10.1016/j.spasta.2024.100847
5. D. Bolin, A. B. Simas, Z. Xiong, Covariance-based rational approximations of fractional SPDEs for computationally efficient Bayesian inference, *J. Comput. Graph. Stat.*, **33** (2024), 64–74. https://doi.org/10.1080/10618600.2023.2231051
6. P. Bossert, Parameter estimation for second-order SPDEs in multiple space dimensions, *Stat. Inference Stoch. Process.*, **27** (2024), 485–583. https://doi.org/10.1007/s11203-024-09318-1
7. A. Chauhan, B. R. Boruah, Study on the orthogonality property of Zernike modes in light beams undergoing free space propagation, *J. Opt. Soc. Am. A*, **40** (2023), 961–968. https://doi.org/10.1364/JOSAA.481741
8. D. Bachmann, M. Isoard, V. Shatokhin, G. Sorelli, A. Buchleitner, Accurate Zernike-corrected phase screens for arbitrary power spectra, *Opt. Eng.*, **64** (2025), 058102. https://doi.org/10.1117/1.OE.64.5.058102
9. E. Goi, S. Schoenhardt, M. Gu, Direct retrieval of Zernike-based pupil functions using integrated diffractive deep neural networks, *Nat. Commun.*, **13** (2022), 2531. https://doi.org/10.1038/s41467-022-35349-4
10. A. B. Siddik, S. Sandoval, D. Voelz, L. E. Boucheron, L. Varela, Estimation of modified Zernike coefficients from turbulence-degraded multispectral imagery using deep learning, *Appl. Opt.*, **63** (2024), E28–E39. https://doi.org/10.1364/AO.521072
11. P. Benner, D. Palitta, J. Saak, On an integrated Krylov-ADI solver for large-scale Lyapunov equations, *Numer. Algor.*, **92** (2023), 35–63. https://doi.org/10.1007/s11075-022-01409-5
12. L. Bao, Y. Lin, Y. Wei, A new projection method for solving large Sylvester equations, *Appl. Numer. Math.*, **57** (2007), 521–532. https://doi.org/10.1016/j.apnum.2006.07.005
13. Y. Lin, Low-rank methods for solving discrete-time projected Lyapunov equations, *Mathematics*, **12** (2024), 1166. https://doi.org/10.3390/math12081166

14. D. Palitta, V. Simoncini, Numerical methods for large-scale Lyapunov equations with symmetric banded data, *SIAM J. Sci. Comput.*, **40** (2018), A3581–A3608. https://doi.org/10.1137/17M1156575
15. A. Andersson, A. Lang, A. Petersson, L. Schroer, Finite element approximation of Lyapunov equations related to parabolic stochastic PDEs, *Appl. Math. Optim.*, **91** (2025), 66. https://doi.org/10.1007/s00245-025-10260-8
16. R. J. Noll, Zernike polynomials and atmospheric turbulence, *J. Opt. Soc. Am.*, **66** (1976), 207–211. https://doi.org/10.1364/JOSA.66.000207
17. N. M. Atakishiyev, G. S. Pogosyan, C. Salto-Alegre, K. B. Wolf, A. Yakhno, The superintegrable Zernike system, In: *Springer proceedings in mathematics & statistics*, Singapore: Springer, **263** (2017), 263–273. https://doi.org/10.1007/978-981-13-2715-5_16
18. D. Zhang, Statistical inference for Ornstein-Uhlenbeck processes based on low-frequency observations, *Stat. Probab. Lett.*, **216** (2025), 110286. https://doi.org/10.1016/j.spl.2024.110286
19. S. Gaïffas, G. Matulewicz, Sparse inference of the drift of a high-dimensional Ornstein-Uhlenbeck process, *J. Multivar. Anal.*, **169** (2019), 1–20. https://doi.org/10.1016/j.jmva.2018.08.005
20. N. Dexheimer, C. Strauch, On Lasso and Slope drift estimators for Lévy-driven Ornstein-Uhlenbeck processes, *Bernoulli*, **30** (2024), 88–116. https://doi.org/10.3150/22-BEJ1574
21. L. Sadek, H. T. Alaoui, The extended nonsymmetric block Lanczos methods for solving large-scale differential Lyapunov equations, *Math. Model. Comput.*, **8** (2021), 526–536.
22. L. Sadek, The methods of fractional backward differentiation formulas for solving two-term fractional differential Sylvester matrix equations, *Appl. Set-Valued Anal. Optim.*, **6** (2024), 137–155. https://doi.org/10.23952/asvao.6.2024.2.02
23. L. Sadek, Control theory for fractional differential Sylvester matrix equations with Caputo fractional derivative, *J. Vib. Control*, **31** (2024), 1586–1602. https://doi.org/10.1177/10775463241246430

A. Proofs for the master energy dissipation framework

A.1. Proof of Proposition 2.1

Under Assumption 2.1 ($\mathcal{L}$ is self-adjoint, dissipative with eigenvalues $\lambda_k \leq -\gamma_0 < 0$) and Assumption 2.2 ($Q$ is positive, self-adjoint trace-class), the unique, positive, self-adjoint steady-state energy covariance operator P exists and is given by the absolutely convergent energy dissipation integral [2, 3]:

$$P = \int_0^\infty e^{\mathcal{L}t} Q e^{\mathcal{L}t} \, \mathrm{d}t. \tag{A.1}$$

To show that this P solves the Lyapunov equation $\mathcal{L}P + P\mathcal{L} = -Q$, we differentiate:

$$\frac{\mathrm{d}}{\mathrm{d}t}(e^{\mathcal{L}t} Q e^{\mathcal{L}t}) = \mathcal{L}e^{\mathcal{L}t} Q e^{\mathcal{L}t} + e^{\mathcal{L}t} Q e^{\mathcal{L}t} \mathcal{L}^*. \tag{A.2}$$

Since $\mathcal{L}$ is self-adjoint, $\mathcal{L}^* = \mathcal{L}$. Integrating from 0 to ∞:

$$[e^{\mathcal{L}t} Q e^{\mathcal{L}t}]_0^\infty = \int_0^\infty (\mathcal{L}e^{\mathcal{L}t} Q e^{\mathcal{L}t} + e^{\mathcal{L}t} Q e^{\mathcal{L}t} \mathcal{L}) \, \mathrm{d}t = \mathcal{L}P + P\mathcal{L}. \tag{A.3}$$

As $t \to \infty$, $e^{\mathcal{L}t} \to 0$ due to the dissipative nature of $\mathcal{L}$ (eigenvalues are negative). At $t = 0$, $e^{\mathcal{L}0} = I$. Thus, $0 - Q = \mathcal{L}P + P\mathcal{L}$, which is $\mathcal{L}P + P\mathcal{L} = -Q$.

To obtain the spectral formula (2.3), we test the Lyapunov equation in the eigenbasis $\{\phi_k\}$ of $\mathcal{L}$:

$$\langle \phi_j, (\mathcal{L}P + P\mathcal{L})\phi_k \rangle = \langle \phi_j, -Q\phi_k \rangle. \tag{A.4}$$

Using $\mathcal{L}\phi_j = \lambda_j \phi_j$ and the self-adjointness of $\mathcal{L}$, we have $\langle \mathcal{L}\phi_j, P\phi_k \rangle = \lambda_j \langle \phi_j, P\phi_k \rangle$ and $\langle \phi_j, P\mathcal{L}\phi_k \rangle = \lambda_k \langle \phi_j, P\phi_k \rangle$. Summing these gives:

$$(\lambda_j + \lambda_k)\langle \phi_j, P\phi_k \rangle = -\langle \phi_j, Q\phi_k \rangle. \tag{A.5}$$

Since $\lambda_j, \lambda_k \le -\gamma_0 < 0$, we have $\lambda_j + \lambda_k < 0$. Therefore, we can divide to get:

$$(P)_{jk} = \frac{\langle \phi_j, Q\phi_k \rangle}{-(\lambda_j + \lambda_k)}, \tag{A.6}$$

where $(P)_{jk} = \langle \phi_j, P\phi_k \rangle$ and $(Q)_{jk} = \langle \phi_j, Q\phi_k \rangle$.

B. Proofs for Zernike geometry

B.1. Proof of Theorem 4.1

The Hilbert space for optical systems on the unit disk is $L^2(D, \mathrm{d}\mu)$, with the normalized area measure $\mathrm{d}\mu = \frac{1}{\pi} r \, \mathrm{d}r \, \mathrm{d}\theta$. In polar coordinates (r, θ), the complex Zernike circle polynomials are $Z_{nm}(r, \theta) = R_n^{|m|}(r) \, e^{\mathrm{i}m\theta}$, where $n \ge |m|$ and $n - |m|$ is even. These form an orthonormal basis.

Consider the differential operator $\mathcal{L}_Z$ defined as:

$$\mathcal{L}_Z f \;=\; -\frac{1}{r}\,\partial_r\Big(r(1-r^2)\,\partial_r f\Big) \;-\; \frac{1}{r^2}\,\partial_{\theta\theta} f. \tag{B.1}$$

This operator acts on functions with the natural boundary condition $\big[(1-r^2)\partial_r f\big]\big|_{r=1} = 0$, which ensures regularity at $r = 1$ (boundary) and at $r = 0$ (center) for Zernike polynomials. Applying this operator to a Zernike mode Z_{nm}:

$$\partial_{\theta\theta} Z_{nm} = -m^2 Z_{nm}. \tag{B.2}$$

For the radial part, we use the well-known radial ODE satisfied by $R_n^{|m|}(r)$ (from its definition as a hypergeometric polynomial transformation, specifically the Jacobi polynomial part):

$$(1 - r^2)\frac{\mathrm{d}^2 R_n^{|m|}}{\mathrm{d}r^2} + \frac{1 - 3r^2}{r}\frac{\mathrm{d}R_n^{|m|}}{\mathrm{d}r} + \Big(n(n+2) - m^2\Big)R_n^{|m|} \;=\; 0. \tag{B.3}$$

The first term for Z_{nm} involves the radial part of $\mathcal{L}_Z$: $-\frac{1}{r}\frac{\mathrm{d}}{\mathrm{d}r}\Big(r(1-r^2)\,\frac{\mathrm{d}R_n^{|m|}}{\mathrm{d}r}\Big) = -\Big((1-r^2)\frac{\mathrm{d}^2 R_n^{|m|}}{\mathrm{d}r^2} + (\frac{1}{r} - 3r)\frac{\mathrm{d}R_n^{|m|}}{\mathrm{d}r}\Big)$. From the radial ODE, we directly have: $(1-r^2)\frac{\mathrm{d}^2 R_n^{|m|}}{\mathrm{d}r^2} + \frac{1-3r^2}{r}\frac{\mathrm{d}R_n^{|m|}}{\mathrm{d}r} = -\Big(n(n+2) - m^2\Big)R_n^{|m|}$. Therefore, substituting this back: $-\frac{1}{r}\frac{\mathrm{d}}{\mathrm{d}r}\Big(r(1-r^2)\,\frac{\mathrm{d}R_n^{|m|}}{\mathrm{d}r}\Big) = (n(n+2) - m^2)R_n^{|m|}$.

Thus, Z_{nm} are eigenfunctions of $\mathcal{L}_Z$ with eigenvalues $\mu_{nm} = n(n+2) - m^2$. Since $n \ge |m|$ and $n - |m|$ is even, we can write $\mu_{nm} = (n - |m|)(n + |m| + 2) \ge 0$. The operator $\mathcal{L}_Z$ is self-adjoint with respect to the inner product $\langle \cdot, \cdot \rangle_\mu$ due to Green's identity and the stated boundary condition, ensuring a real spectrum and orthonormal eigenbasis. Finally, the full dissipative operator is $\mathcal{L} = -\alpha^2 \mathcal{L}_Z - \gamma I$. Its eigenvalues are $\lambda_{nm} = -\alpha^2 \mu_{nm} - \gamma$. Since $\alpha^2 > 0$, $\gamma > 0$, and $\mu_{nm} \ge 0$, it follows that $\lambda_{nm} \le -\gamma < 0$, satisfying Assumption 2.1. The piston mode ($n = 0, m = 0$) has $\mu_{00} = 0$, yielding the least negative eigenvalue $\lambda_{00} = -\gamma$.

B.2. Proof of Theorem 4.2 (Structure of Q in the Zernike basis)

The matrix elements of the noise operator Q in the Zernike basis are given by:

$$(Q)_{jk} \;=\; \langle Z_j, QZ_k\rangle_\mu \;=\; \iint_{D\times D} Z_j(\mathbf{x})\, C(\mathbf{x},\mathbf{x}')\, Z_k(\mathbf{x}')\, \mathrm{d}\mu(\mathbf{x})\, \mathrm{d}\mu(\mathbf{x}'). \tag{B.4}$$

For atmospheric turbulence following the Kolmogorov model, the spatial phase covariance function $C(\mathbf{x},\mathbf{x}')$ (for circular apertures and statistically isotropic conditions) is rotationally invariant. This means $C(\mathbf{x},\mathbf{x}')$ depends only on r, r' and the angular difference $\Delta\theta = \theta - \theta'$, and not on the absolute angles θ, θ'. Therefore, $C(r, r', \Delta\theta)$ can be expanded in a Fourier series:

$$C(r, r', \Delta\theta) \;=\; \sum_{\ell\in\mathbb{Z}} c_\ell(r, r')\, e^{\mathrm{i}\ell(\theta-\theta')}. \tag{B.5}$$

Substitute $Z_j(r,\theta) = R_{n_j}^{|m_j|}(r)\, e^{\mathrm{i}m_j\theta}$ and $Z_k(r',\theta') = R_{n_k}^{|m_k|}(r')\, e^{\mathrm{i}m_k\theta'}$, and integrate over θ and θ':

$$\begin{aligned}
&\iint_0^{2\pi}\int_0^{2\pi} Z_j(r,\theta) C(r,r',\Delta\theta) Z_k(r',\theta')\ \mathrm{d}\theta\ \mathrm{d}\theta' \qquad (B.6)\\
&= \iint_0^{2\pi}\int_0^{2\pi} R_{n_j}^{|m_j|}(r) e^{\mathrm{i}m_j\theta} \sum_{\ell\in\mathbb{Z}} c_\ell(r,r')\, e^{\mathrm{i}\ell(\theta-\theta')} R_{n_k}^{|m_k|}(r') e^{\mathrm{i}m_k\theta'}\ \mathrm{d}\theta\ \mathrm{d}\theta'\\
&= R_{n_j}^{|m_j|}(r) R_{n_k}^{|m_k|}(r') \sum_{\ell\in\mathbb{Z}} c_\ell(r,r') \left(\int_0^{2\pi} e^{\mathrm{i}(m_j+\ell)\theta}\ \mathrm{d}\theta\right)\left(\int_0^{2\pi} e^{\mathrm{i}(m_k-\ell)\theta'}\ \mathrm{d}\theta'\right).
\end{aligned}$$

The angular integrals are non-zero only if $m_j+\ell = 0$ and $m_k-\ell = 0$, which implies $\ell = -m_j$ and $\ell = m_k$. Therefore, $m_j = m_k$. If $m_j \neq m_k$, then $(Q)_{jk} = 0$. This confirms the first condition (block-diagonal in m).

For a fixed $m_j = m_k = m$, the expression for $(Q)_{jk}$ becomes (after normalizing for $\mathrm{d}\mu$):

$$(Q)_{jk} \;=\; \frac{1}{\pi^2}\int_0^1\int_0^1 R_{n_j}^{|m|}(r) c_m(r,r') R_{n_k}^{|m|}(r')\, r\,\mathrm{d}r\, r'\,\mathrm{d}r'. \tag{B.7}$$

For statistically isotropic Kolmogorov turbulence, Noll's derivations show that the radial covariance function $c_m(r,r')$ is highly structured. While the general theory does not universally demand vanishing integrals purely based on radial index parity for all m, specific forms of $c_m(r,r')$ lead to significant decay or even orthogonality for modes with different parity or large index differences. Thus, for practical applications, the coupling between modes with significantly different radial degrees (for a fixed m) or different parities is often negligible, especially for higher modes, consistent with the description of Q having a structured sparse form and coupling primarily for lower modes.

C. Proofs for the OU extension

C.1. Proof of Theorem 5.1

We analyze the stochastic system:

$$\dot{x}(t) = \mathcal{L}x(t) + \eta(t), \tag{C.1}$$

$$\mathrm{d}\eta(t) = -\tau^{-1}\eta(t)\ \mathrm{d}t + \sqrt{2\tau^{-1}}\, Q^{1/2}\ \mathrm{d}W_t.$$

Let $z(t) := \begin{bmatrix} x(t) \\ \eta(t) \end{bmatrix}$ be the augmented state. The system can be written as:

$$\mathrm{d}z(t) = \mathbb{A}z(t)\ \mathrm{d}t + \mathbb{G}\ \mathrm{d}W_t, \tag{C.2}$$

where

$$\mathbb{A} = \begin{bmatrix} \mathcal{L} & I \\ 0 & -\tau^{-1}I \end{bmatrix}, \quad \mathbb{G} = \begin{bmatrix} 0 \\ \sqrt{2\tau^{-1}}\, Q^{1/2} \end{bmatrix}. \tag{C.3}$$

The unique steady-state covariance $\mathbb{P} = \mathbb{E}[zz^*]$ solves the augmented Lyapunov equation:

$$\mathbb{A}\,\mathbb{P} + \mathbb{P}\,\mathbb{A}^* + \mathbb{G}\mathbb{G}^* = 0. \tag{C.4}$$

Let $\mathbb{P}$ be partitioned as $\mathbb{P} = \begin{bmatrix} P_{xx} & P_{x\eta} \\ P_{\eta x} & P_{\eta\eta} \end{bmatrix}$. The term $\mathbb{G}\mathbb{G}^*$ is $\begin{bmatrix} 0 & 0 \\ 0 & 2\tau^{-1}Q \end{bmatrix}$. Substituting these blocks into the Lyapunov equation gives the following system of operator equations:

$$\mathcal{L}P_{xx} + P_{xx}\mathcal{L}^* + P_{x\eta} + P_{\eta x} = 0, \tag{C.5}$$
$$\mathcal{L}P_{x\eta} + P_{x\eta}(-\tau^{-1}I) + P_{\eta\eta} = 0, \tag{C.6}$$
$$(-\tau^{-1}I)P_{\eta\eta} + P_{\eta\eta}(-\tau^{-1}I) + 2\tau^{-1}Q = 0. \tag{C.7}$$

We solve this system sequentially:

(1) From Eq (C.7): $-2\tau^{-1}P_{\eta\eta} + 2\tau^{-1}Q = 0 \implies P_{\eta\eta} = Q$. This confirms that Q is indeed the stationary covariance of η.

(2) From Eq (C.6), we substitute $P_{\eta\eta} = Q$: $\mathcal{L}P_{x\eta} - \tau^{-1}P_{x\eta} = -Q$. This is an operator Sylvester equation $(\mathcal{L} - \tau^{-1}I)P_{x\eta} = -Q$. Since $\mathcal{L}$ is self-adjoint with eigenvalues λ_j and I commutes with $\mathcal{L}$, we can express the solution in the eigenbasis:

$$(\lambda_j - \tau^{-1})(P_{x\eta})_{jk} = -(Q)_{jk} \implies (P_{x\eta})_{jk} = \frac{-(Q)_{jk}}{\lambda_j - \tau^{-1}}. \tag{C.8}$$

Since $P_{\eta x} = P_{x\eta}^*$, we have $(P_{\eta x})_{jk} = \overline{(P_{x\eta})_{kj}} = \frac{-\overline{(Q)_{kj}}}{\overline{\lambda_k} - \tau^{-1}}$. Assuming Q and $\mathcal{L}$ are real for simplicity, $(P_{\eta x})_{jk} = \frac{-(Q)_{kj}}{\lambda_k - \tau^{-1}}$. If Q is symmetric, then $(Q)_{jk} = (Q)_{kj}$.

(3) Substitute $P_{x\eta}$ and $P_{\eta x}$ into Eq (C.5): $\mathcal{L}P_{xx} + P_{xx}\mathcal{L}^* = -(P_{x\eta} + P_{x\eta}^*)$. In the eigenbasis, for j, k:

$$(\lambda_j + \lambda_k)(P_{xx})_{jk} = -\left(\frac{-(Q)_{jk}}{\lambda_j - \tau^{-1}} + \frac{-(Q)_{kj}}{\lambda_k - \tau^{-1}}\right). \tag{C.9}$$

If $\mathcal{L}$ and Q are real-valued (as is the case for Zernike systems when Z_j are real, and Kolmogorov Q in the standard Noll basis), then $(Q)_{kj} = (Q)_{jk}$:

$$(\lambda_j + \lambda_k)(P_{xx})_{jk} = (Q)_{jk}\left(\frac{1}{\lambda_j - \tau^{-1}} + \frac{1}{\lambda_k - \tau^{-1}}\right) = (Q)_{jk}\frac{\lambda_k - \tau^{-1} + \lambda_j - \tau^{-1}}{(\lambda_j - \tau^{-1})(\lambda_k - \tau^{-1})}. \tag{C.10}$$

Therefore,

$$(P_{xx})_{jk} = \frac{(Q)_{jk}}{(\lambda_j + \lambda_k)} \frac{\lambda_j + \lambda_k - 2\tau^{-1}}{(\lambda_j - \tau^{-1})(\lambda_k - \tau^{-1})}. \tag{C.11}$$

This can be rewritten using the modal dissipation rates $\delta_j = -\lambda_j > 0$:

$$(P_{xx})_{jk} = \frac{(Q)_{jk}}{(\delta_j + \delta_k)} \frac{-(\delta_j + \delta_k) - 2\tau^{-1}}{(-\delta_j - \tau^{-1})(-\delta_k - \tau^{-1})} = \frac{(Q)_{jk}}{-(\delta_j + \delta_k)} \frac{(\delta_j + \delta_k + 2\tau^{-1})}{(\delta_j + \tau^{-1})(\delta_k + \tau^{-1})}. \tag{C.12}$$

Or, using $-\lambda_j$ as in the theorem statement:

$$(P_{xx})_{jk} = \frac{(Q)_{jk}}{(-\lambda_j)(-\lambda_k)} \cdot \frac{(-\lambda_j - \lambda_k + 2\tau^{-1})}{((-\lambda_j + \tau^{-1})(-\lambda_k + \tau^{-1}))}. \tag{C.13}$$

For diagonal Q, where $j = k$, we have $(P_{xx})_{jj} = \frac{(Q)_{jj}}{(-\lambda_j)(-\lambda_j + \tau^{-1})}$, as given in Eq (5.3).

D. Proofs of error bounds

D.1. Proof of Theorem 6.1

Let P be the exact covariance operator and $P_N = \Pi_N P \Pi_N$ its N-mode projection, where Π_N is the orthogonal projection onto $\text{span}\{Z_1, \ldots, Z_N\}$. The error operator is $E_N = P - P_N$. In the Zernike basis, $P_{jk} = (Q)_{jk}/(\alpha^2(\mu_j + \mu_k) + 2\gamma)$.

(1) *Exactly diagonal noise:* If Q is diagonal, $(Q)_{jk} = q_j \delta_{jk}$, and then P is also diagonal: $(P)_{jk} = P_{jj}\delta_{jk} = \frac{q_j}{2(\alpha^2\mu_j + \gamma)}\delta_{jk}$. The operator P_N keeps the first N diagonal entries, i.e., $(P_N)_{jj} = P_{jj}$ for $j \le N$ and $(P_N)_{jj} = 0$ for $j > N$. The error operator $P - P_N$ has entries $(P - P_N)_{jj} = 0$ for $j \le N$ and $(P - P_N)_{jj} = P_{jj}$ for $j > N$. The operator norm of a diagonal operator is the supremum of its diagonal entries:

$$\|P - P_N\|_{\text{op}} = \sup_{j>N} |(P - P_N)_{jj}| = \sup_{j>N} P_{jj} = \sup_{j>N} \frac{q_j}{2(\alpha^2\mu_j + \gamma)}. \tag{D.1}$$

This proves Eq (6.2).

(2) *Structured noise with diagonal dominance:* For general Q, the operator $P - P_N$ can be decomposed into three blocks corresponding to the truncation:

$$P - P_N = \Pi_N P \Pi_N^{\perp} + \Pi_N^{\perp} P \Pi_N + \Pi_N^{\perp} P \Pi_N^{\perp}, \tag{D.2}$$

where $\Pi_N^{\perp} = I - \Pi_N$. For many physical systems (such as Kolmogorov turbulence as discussed in Theorem 4.2), the noise operator Q is sparse or rapidly decaying away from the diagonal in the Zernike basis. This structured nature of Q (e.g., block-diagonal or band-diagonal after sorting) leads to P also exhibiting similar spectral properties. In such cases, off-diagonal terms involving $\Pi_N P \Pi_N^{\perp}$ (coupling modes below N with modes above N) and $\Pi_N^{\perp} P \Pi_N$ are generally smaller and decay faster than diagonal terms. Thus, the operator norm error is predominantly set by $\Pi_N^{\perp} P \Pi_N^{\perp}$, whose entries are P_{jk} for $j, k > N$. The largest entries in this block are typically the diagonal ones:

$$\|P - P_N\|_{\text{op}} \approx \|\Pi_N^{\perp} P \Pi_N^{\perp}\|_{\text{op}} = \sup_{j>N, k>N} |\langle Z_j, P Z_k \rangle|. \tag{D.3}$$

For a sufficiently diagonally dominant Q (in the sense that $\sum_{k\neq j}|Q_{jk}| \ll q_j$), the largest elements are $(P)_{jj}$. Therefore, we obtain the practical bound in Eq (6.4). This assumes that q_j provides the dominant scale of elements for $j > N$. The term $\min_{j>N}(\alpha^2\mu_j + \gamma)$ provides the smallest denominator among the modes excluded, controlling the upper bound. The minimum eigenvalue $\mu_{N+1}^{\min}$ refers to the smallest μ_j among $j > N$. As shown in Remark 6.1, $\mu_{N+1}^{\min} \sim C_\mu\sqrt{N}$.

(3) *Convergence rates:* Substituting $\mu_j \sim C_\mu\sqrt{j}$ into the bound:

$$\|P - P_N\|_{\text{op}} \lesssim \frac{\sup_{j>N} q_j}{2(\alpha^2 C_\mu\sqrt{N+1} + \gamma)}. \tag{D.4}$$

- If q_j is bounded (e.g., $q_j \approx C$): The convergence is $O(N^{-1/2})$.
- For $q_j \sim j^{-p}$: The convergence is $O(N^{-p}N^{-1/2}) = O(N^{-(p+1/2)})$.
- For Kolmogorov turbulence, $(Q)_{jj}$ modes with $n_j > 1$, excluding piston/tilt, scale as $(n_j(n_j + 1))^{-11/6}$ in a similar way as with to Noll [16]. Using the simpler scaling from Noll, the RMS values for Zernike mode coefficients $\langle a_j^2\rangle$ for Kolmogorov fall off as $(n_j)^{-11/3}$ for $n_j > 1$. So, $q_j \sim n_j^{-11/3}$. Given $n_j \sim \sqrt{j}$ for the cumulative index, $q_j \sim (\sqrt{j})^{-11/3} = j^{-11/6}$. Therefore, $p = 11/6$. The convergence rate for Kolmogorov turbulence becomes $O(N^{-(11/6+1/2)}) = O(N^{-(11/6+3/6)}) = O(N^{-14/6}) = O(N^{-7/3})$.

D.2. Proof of Theorem 6.2

The Hilbert-Schmidt norm of an operator A is defined as $\|A\|_{\text{HS}}^2 = \sum_{j,k}|(A)_{jk}|^2$ in an orthonormal basis. Let $E_N = P - \Pi_N P\Pi_N$ be the approximation error. In the Zernike basis, the matrix elements of E_N are:

$$(E_N)_{jk} = \begin{cases} 0 & \text{if } j \le N \text{ and } k \le N, \\ (P)_{jk} & \text{if } j > N \text{ or } k > N. \end{cases} \tag{D.5}$$

Thus, the Hilbert-Schmidt norm squared is:

$$\|P - P_N\|_{\text{HS}}^2 = \sum_{\substack{j,k\in\mathbb{N} \\ (j\le N\wedge k>N)\vee(j>N\wedge k\le N)\vee(j>N\wedge k>N)}} |(P)_{jk}|^2. \tag{D.6}$$

Substituting the spectral form of $(P)_{jk} = \frac{(Q)_{jk}}{(\alpha^2(\mu_j+\mu_k)+2\gamma)}$, we get:

$$\|P - P_N\|_{\text{HS}}^2 = \sum_{\substack{j,k\in\mathbb{N} \\ (j\le N\wedge k>N)\vee(j>N\wedge k\le N)\vee(j>N\wedge k>N)}} \frac{|(Q)_{jk}|^2}{(\alpha^2(\mu_j+\mu_k)+2\gamma)^2}. \tag{D.7}$$

This explicitly proves Eq (6.6).

For the practical bound in Eq (6.8), let $\Omega_N = \{(j,k) : \max(j,k) > N\}$. This is the set of indices for terms remaining in $P - P_N$. For any $(j,k) \in \Omega_N$, at least one index is greater than N. Therefore:

$$\mu_j + \mu_k \ge \mu_{N+1}^{\min} + \mu_1 \quad \text{or} \quad \mu_j + \mu_k \ge \mu_1 + \mu_{N+1}^{\min} \quad \text{or} \quad \mu_j + \mu_k \ge 2\mu_{N+1}^{\min}. \tag{D.8}$$

More generally, $\min_{\max(j,k)>N}(\mu_j + \mu_k) \ge \mu_{N+1}^{\min}$ (considering j or k minimums). The denominator for any $(j,k) \in \Omega_N$ is lower-bounded by $2\gamma + \alpha^2\mu_{N+1}^{\min}$.

Thus, we can bound the sum by using the minimum possible value for the denominator term $\alpha^2(\mu_j + \mu_k) + 2\gamma$ for $(j,k) \in \Omega_N$. This minimum is bounded by $\alpha^2\mu_{N+1}^{\min} + 2\gamma$ (occurring for (j,k), where one index is $N+1$ and the other is 00, with $\mu_{00} = 0$, or even for $2\alpha^2\mu_{N+1}^{\min} + 2\gamma$ if both $j,k > N$). Using the conservative lower bound $\alpha^2\mu_{N+1}^{\min} + 2\gamma$:

$$\|P - P_N\|_{\text{HS}}^2 \leq \frac{1}{(\alpha^2\mu_{N+1}^{\min} + 2\gamma)^2} \sum_{(j,k)\in\Omega_N} |(Q)_{jk}|^2. \tag{D.9}$$

Let $\|Q_{rest}\|_{\text{HS}}^2 = \sum_{(j,k)\in\Omega_N} |(Q)_{jk}|^2$. This yields the bound:

$$\|P - P_N\|_{\text{HS}} \leq \frac{1}{\alpha^2\mu_{N+1}^{\min} + 2\gamma} \|Q_{rest}\|_{\text{HS}}. \tag{D.10}$$

As discussed in Remark 6.1, $\mu_{N+1}^{\min} \sim C_\mu \sqrt{N}$. If the norm of the truncated part of Q, $\|Q_{rest}\|_{\text{HS}}$, decays as $O(N^{-\beta})$ (which is typical for smooth noise kernels with decaying power in higher modes), then the overall convergence rate is:

$$\|P - P_N\|_{\text{HS}} \sim O(N^{-1/2} \cdot N^{-\beta}) = O(N^{-(1/2+\beta)}). \tag{D.11}$$

AIMS Press